Regular Paper
J. Korean Inst. Electr. Electron. Mater. Eng.
Vol. 33, No. 5, pp. 380-385 September 2020
DOI: https://doi.org/10.4313/JKEM.2020.33.5.380
ISSN 1226-7945(Print), 2288-3258(Online)

Design and Analysis of Small Walking Robots Utilizing Piezoelectric Benders

Jong Man Park, Chi Hoon Song, and Min Ho Park

Defense Agency for Technology and Quality, Jinju 52851, Korea

(Received June 27, 2020; Revised July 26, 2020; Accepted July 28, 2020)

Abstract: Over the past decade, small robots have been of particular interest in the engineering field. Among the various types of small robots, biomimetic robots, which mimic animals and insects, have been developed for special activities in areas where humans cannot physically access. The optimal motion of a walking robot can be determined by the characteristics of the traversed surface (e.g., roughness, curvature, slope, materials, etc.). This study proposes three types of piezoelectric structures using different driving mechanisms, depending on the application range of the small walking robots. Dynamic modeling using computer-aided engineering optimized the shape of the robot to maximize its moving characteristics, and the results were also verified through its fabrication and experimentation. Three types of robots, named by their actuator shapes as I, π, & T-shape, were proposed regarding application for small scale ambulatory robots to different terrain conditions. Among these, the T-shaped robots were shown to have a wide range of speeds (from 2 mm/s up to 255 mm/s) and good carrying capacity (up to 10 g at 50 mm/s) through driving experiments. Based on this study, we proposed possible application areas for the three types of walking robot actuators.

Keywords: Ambulatory robot, Biomimetic robot, Piezoelectric actuator.

1. INTRODUCTION

The start of the biomimetic robotics began by observing the movement of the living body and imitating its movements. Especially, it can be found from various attempts of locomotion means. After the wheel was invented, the wheel was indeed responsible for the revolutionary work as a means of transportation. However, the actual accessible area of the wheel is limited to obstacles less than half the height of a well-worn road or wheel [1,2]. To overcome these problems, there is a growing interest in mechanisms that can move freely like organisms. Biomimetic robots are born with this interest and they have been studied to overcome limitations [3,4].

Piezoelectric actuators are in the spotlight as a driving source for microrobotic applications due to high bandwidth, high power density, and the ability to scale to small sizes. However, the main disadvantage of either stack or cantilever piezoelectric actuators are small displacement [5,6].

In this study, using piezoelectric ceramic benders with low-occurring displacement, it proposed biomimetic robot actuators that overcome the shortcomings by optimizing the structure and imitating the movements of insects. Three types of actuators which were named by their shapes as I, π & T-shape actuators for small scale ambulatory robots were proposed regarding applications for the different terrain conditions.

✉ **Min Ho Park; maxmino@naver.com**

Copyright ©2020 KIEEME. All rights reserved.
This is an Open-Access article distributed under the terms of the Creative Commons Attribution Non-Commercial License (http://creativecommons.org/licenses/by-nc/3.0) which permits unrestricted non-commercial use, distribution, and reproduction in any medium, provided the original work is properly cited.

2. RESEARCH METHOD

2.1 Process of fabrication and materials

Three types of piezoelectric actuators were manufactured based on the results obtained by finite element analysis. The piezoelectric ceramics in the polarization state (Table 1) were cut to fit the size of the elastic body, and carbon fiber was used as the elastic body. Epoxy bond (EPO-TEK, 353ND) was applied between the piezoelectric ceramic and the elastic body and then heated in a heating furnace at 120℃ for 30 minutes to conduct high-temperature curing. To minimize the effects of epoxy bonds, the epoxy layer was applied as thinly as possible to areas where the elastomer and the ceramic contacted each other, and a strong compression was applied during the curing process. In the process of transmitting the vibration of the piezoelectric ceramic to the elastic body, it is also a part requiring strong adhesion to prevent the piezoelectric ceramic from falling. The finished piezoelectric bender was connected to the power supply line, and joints and tips were bonded to each connection part with epoxy bonds.

Table 1. Parameters of piezoceramic materials (PIC151, Physik Instrumente GmbH & Co.).

Physical and dielectric properties		Unit	PIC151
Density		g/cm^3	7.80
Curie temperature		℃	250
Relative permittivity	in the polarization direction	-	2,400
	⊥ to polarity	-	1,980
Dielectric loss factor		10^{-3}	20
Piezoelectric voltage coefficient	d_{31} [pm/v]	-	-210
	d_{33} [pm/v]	-	500
Mechanical quality factor	Q_m	-	100

3. RESULTS AND DISCUSSIONS

3.1 I-shape robot actuator

An I-shape robot actuator utilizing a smooth impact drive mechanism (SIDM) was proposed. It is easy to fabricate an actuator because of the simple structure of a bimorph type piezoelectric ceramic cantilever without any rotators or sliders. The cantilever, called as the leg, was composed of four rectangular ceramics that were attached on the surfaces of an elastic body. Computer-aided engineering, a finite-element analysis (FEA), was used to optimize the driving characteristics of the actuator. Figure 1 shows the structure and parameters for the simulation.

To estimate the speed of the actuator, we assumed as $S_a = d_p \times f_r$, where S_a, d_p and f_r are speed of the actuator, displacement of the pod, and resonance frequency respectively. Summary of the FEA results are as follows, the wider legs (5 mm) and stainless steel (SUS) for the material of legs had better speed, the length of piezoelectric ceramics at 15 mm (equal to the length of legs) had highest speed, and the bimorph was faster than the unimorph. There were the acceptable differences between FEA and experiments [7]. The SIDMs have been practically applied in-camera modules and cellular phones due to their precise positioning ability and compact size. The principle of SIDM is a stick-slip motion achieved by a saw-tooth like the movement of the multi-layered piezoelectric ceramic. In addition, SIDM was adopted to swing the image sensor in image stabilization systems so as to compensate for the human's handshake [8]. The displacement of the actuator is proportional to the time period in which it slides. And the time can be controlled by the duty cycle of the bipolar rectangular wave. The actuator is driven by two successive motions as shown

(a)

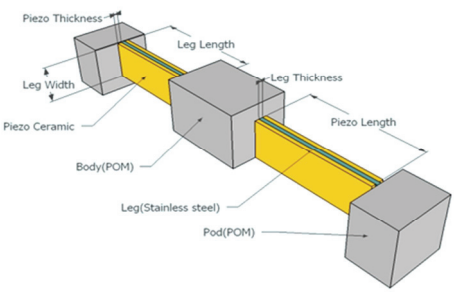

(b)

Parameters				
Leg width(a)	2.0mm	3.0mm	4.0mm	5.0mm
Leg material(b)	Aluminum	Brass	Cooper	Stainless steel
Piezo ceramic length(c)	3.5mm	4.0mm	4.5mm	5.0mm
Piezo ceramic layer(d)	Unimorph	Bimorph		

Fig. 1. (a) Schematic structure and (b) parameters for simulation of I-shape robot actuator.

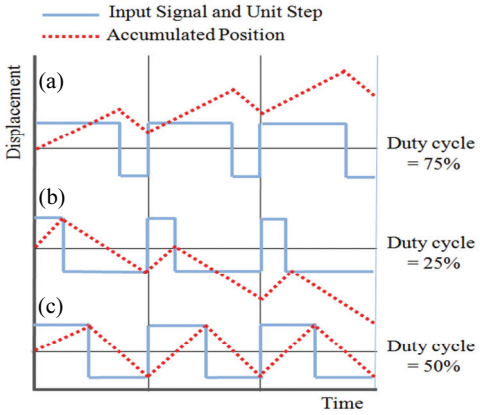

Fig. 2. Actuator sliding characteristics depending on duty cycle: (a) duty cycle 75%, (b) duty cycle 25%, and (c) duty cycle 50%.

in Fig. 2. At duty cycle, 75% in (a), the sliding time (75% of the period of the driving wave) in the forward motion is longer than the backward motion (25% of the period), and consequently, the actuator shall move to forward direction. In the same manner, at the duty cycle, 25% in (b), the actuator shall move to a backward direction. In the case of duty cycle 50% in (c), the sliding time of both directions is the same, and the actuator position shall be almost the same.

After the fabrication of the actuator, the vibration characteristics were measured by laser Doppler Vibrometer (OVF-5000, Polytec). When a bipolar rectangular wave which has a different duty cycle at resonance frequency was applied, the piezoelectric actuator was moved by a stick-slip driving mechanism. Figure 3 shows the vibrations of actuator synchronized to input voltages (78 Vpp, 5 Hz (a) duty cycle 25%, and (b) duty cycle 75%). The displacement (green line, step distance) of the actuator by a pulse (blue line) was approximately one micrometer. The step distance can be accumulated by repeating the cycle of input voltages for a large distance. The moving direction of the actuator can be controlled by the duty cycle of driving signals. When the duty cycle of signals was lower than 50% [see Fig. 3(a), duty cycle 25%], the actuator was moved backward. In the inverse case [see Fig. 3(b), duty cycle 75%], the actuator was moved forward. At off-resonant frequency (5 Hz), the step displacement of the actuator by each pulse (step distance) was 1 μm and the continuous moving speed was 5 mm/sec.

Figure 4 shows the movement of the actuator under the

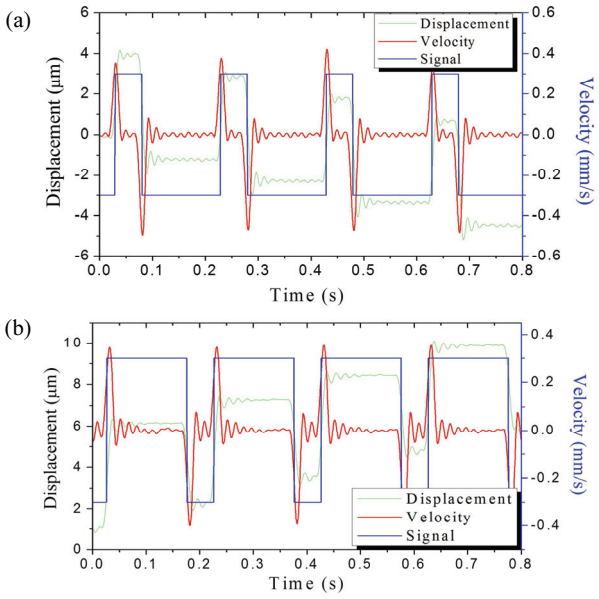

Fig. 3. Displacements at (a) duty cycle 25% and (b) duty cycle 75%.

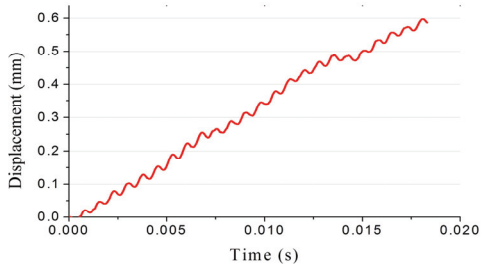

Fig. 4. Displacements at frequency (1,330 Hz, duty cycle 75%).

continuous driving conditions at resonant frequency (1,330 Hz, 40 Vpp, duty cycle 75%). The movement was measured at the center of the body. The stick-slip motions were achieved by a saw-tooth like movement which was driven by two successive motions of the actuator, slow forward and rapid backward movement. At resonant frequency (1,330 Hz), the step distance was 27 mm and the continuous moving speed was up to 33 mm/sec.

3.2 π-shape shape robot actuator

A π-shape actuator proposed a linear displacement drive system utilizing the elliptical motion on the two tips of the actuator. It is easy to assemble the actuator with a modular type because of the simple structure of piezoelectric benders. The modular type actuators of a segmented myria-

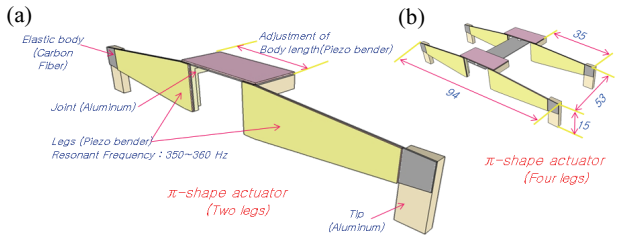

Fig. 5. (a) Structure of π-shape actuator and (b) demensions of the segmented myriapods robot [unit: mm].

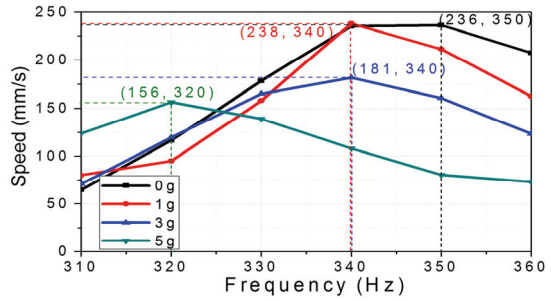

Fig. 7. FEA result of resonance frequency regarding body length.

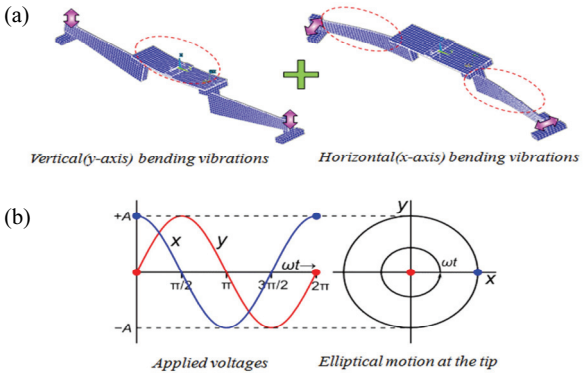

Fig. 6. (a) Vertical and horizontal bending vibration of π-shape actuator and (b) applied voltage and elliptical motions of π-shape robot actuator.

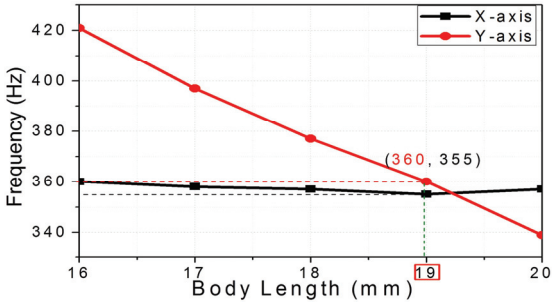

Fig. 8. FEA result of displacement regarding frequency.

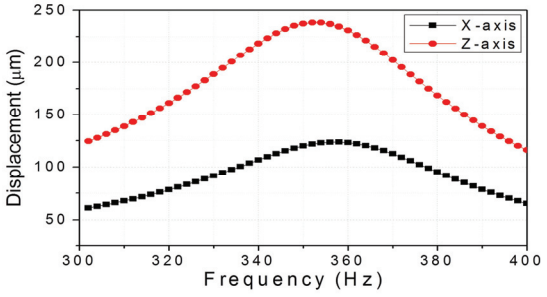

Fig. 9. Speed depending on frequency and load.

pods robot could be added and removed for different tasks or performances as shown in Fig. 5(a) and (b). A π-shape structure was composed of three piezoelectric ceramic benders: one of the benders was positioned on the center of the actuator and joint parts were attached at the ends of the cantilever. The other two benders were positioned on the side of the actuator and were attached between the joint and the tips.

The actuator structure was designed to obtain the 1st bending mode of the horizontal vibration and the vertical vibration at the same frequency, when two sinusoidal wave voltages with a 90° phase difference were applied to two pairs of the actuator benders, elliptical motions were obtained at the tips [9,10]. The ANSYS, a finite-element analysis program was used to find the optimal structure of piezoelectric bender which has maximum mechanical energy-weight ratio and frequency matching between horizontal and vertical vibrations. (see Fig. 6)

As in Fig. 7, resonant frequencies for y-axis vibration were linearly decreased depending on the increasing length of the body, however, the resonant frequencies for x-axis vibration were almost invariable. At the cross point, the vertical and horizontal vibrations occurred at the same frequency. Length of 30 mm was determined by the FEA. In Fig. 8, the maximum displacement of the x-axis was found at 350~360 Hz and the maximum displacement of the y-axis was found at 355 Hz.

As a result of FEA, A π-shape robot actuator was assembled and the speed was measured with placing on an acrylic plastic plate. As in Fig. 9, the maximum speed of 236 mm/sec. was obtained at 350 Hz, 30

Vrms. When the load of the robot was increased by putting weight mass on the center of the actuator, speed and the maximum speed frequency of the robot were decreased up to 320 Hz at 155 mm/sec.

3.3 T-shape shape robot actuator

A T-shape robot actuator is proposed as a biomimetic robot driving source using piezoelectric ceramics. It is suggested that a rougher ground plane can be used as an alternative to the above two robot driving sources. By creating elliptical displacements in the legs connected by pin joint and the slotted hole in two orthogonal moments, the ability to overcome obstacles on the moving surface is increased. The T-shaped structure was designed for the 1st bending mode of the horizontal vibration and the vertical vibration to have the same frequency in order to obtain elliptical motion at the legs using a pin joint.

In order to make the motion of the biomimetic robot legs similar to the movements of the cockroaches, two pairs of legs in the diagonal direction in the four-leg structures are required to make the same movement as shown in the Fig. 11. The polarization direction of the piezoelectric ceramics is different from each other in a pair of legs as shown in Fig. 12(a). The power source connection and applied are shown in Fig. 12(b). In order to make continuous movement in one direction, the position of the leg is determined according to the order of the applied voltage with a 90° phase difference as shown in the Fig. 11.

A T-shape robot actuator was assembled and its driving characteristics were measured with placing on different roughness surfaces. As shown in Fig. 13(a), Similar to the displacement measurement results was confirmed that the speed increases with increasing frequency and applied voltage. The maximum speed was 266 mm/sec, when applied 90 Vrms at 40 Hz. In addition, the speed decreased from 50 Hz, and the speed decreased remarkably above 60 Hz. And the speed decreased as the load increased up to 10 g, it was confirmed that the driving characteristics remarkably decreased from over 8 g. In order to understand the speed characteristics according to the roughness of the moving surface, the speed according to the driving frequency was measured on the sandpaper of different roughness (from P220 to P60) and the result as shown in the Fig. 13(b) was obtained.

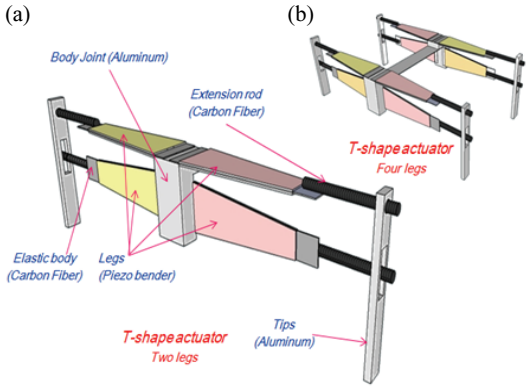

Fig. 10. (a) Structure of T-shape robot actuator and (b) the segmented myriapods robot.

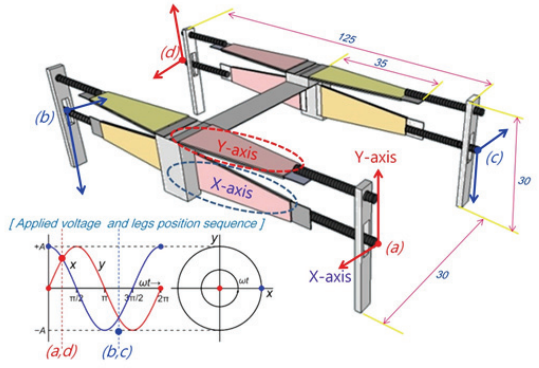

Fig. 11. Applied voltage sequence and dimensions of T shape robot actuator [unit: mm].

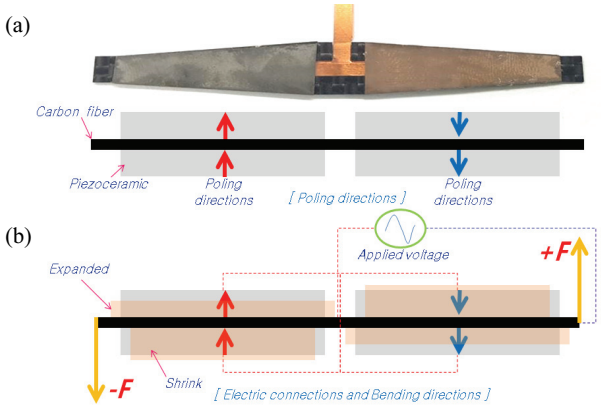

Fig. 12. (a) Poling and assembling direction of piezoceramic bender and (b) electric connections and bending direction of bender.

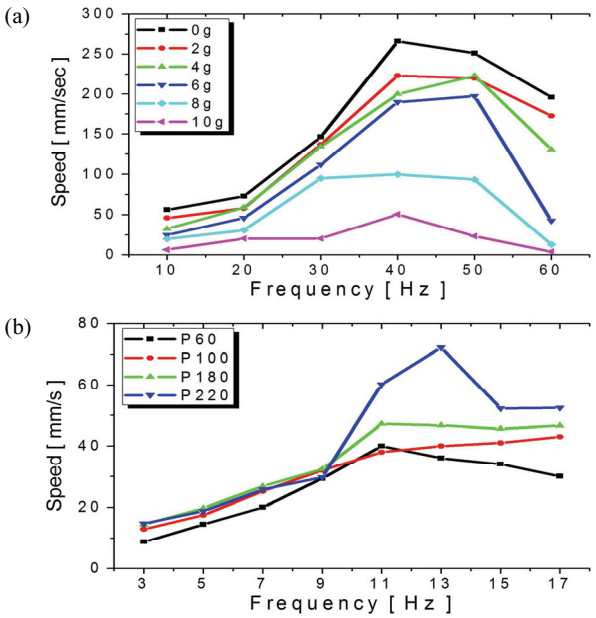

Fig. 13. (a) Speed of the T-shape robot actuator depending on frequency and load and (b) roughness of surface.

4. CONCLUSION

In this paper, we propose newly designed three types of piezoelectric actuators for driving a small scale (from a few cubic centimeters up to several hundred cubic centimeters) ambulatory robots (See Fig. 14). The optimal driving form of the walking robot can be determined by the characteristics of the moving surface (e.g., roughness, curvature, slope, materials, etc.). Table 2 shows the suggestion of an applicable area of three types of ambulatory robot actuators. The I-shape robot actuator moves on a very smooth surface for precise positioning on the order of a few micrometers with fast movement. The π-shape robot actuator can travel on indoor floors for such as small spy robot with very fast speed. Lastly, the T-shape robot actuator can move more rough floors or even outdoor, such as paved roads, and climb gradient floors for such as ambulatory spy robots.

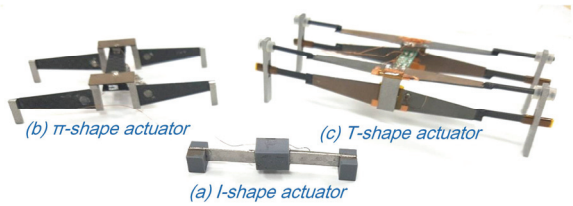

Fig. 14. The tested models of I, π, T-shape robot actuator.

Table 2. Suggestion of applicable area.

Autuators	I-shape	π-shape	T-shape
Floor conditions	Smooth	Medium	Rough
Sand paper grade [Grit diameter (㎛)]	P2000 (~12 ㎛)	P340 (~40 ㎛)	P60 (~269 ㎛)
Applicable for	Precise stages	Spy robot	Spy robot

ORCID

Min Ho Park https://orcid.org/0000-0001-9241-7978

REFERENCES

[1] P. Dario, R. Valleggi, M. C. Carrozza, M. C. Montesi, and M. Cocco, *J. Micromech. Microeng.*, **2**, 141 (1992). [DOI: https://doi.org/10.1088/0960-1317/2/3/005]

[2] K. Spanner, White Paper for Actuator (2006).

[3] S. Avadhanula and R. S. Fearing, *Proc. 2005 IEEE International Conference on Robotics and Automation* (IEEE, Barcelona, Spain, 2005) p. 1579. [DOI: https://doi.org/10.1109/ROBOT.2005.1570339]

[4] R. J. Wood, S. Avadhanula, R. Sahai, E. Steltz, and R. S. Fearing, *J. Mech. Des.*, **130**, 052304 (2008). [DOI: https://doi.org/10.1115/1.2885509]

[5] D. Campolo, R Sahai, and R. S. Fearing, *Proc. 2003 IEEE International Conference on Robotics and Automation (Cat. No.03CH37422)* (Taipei, Taiwan, 2003) p. 3339. [DOI: https://doi.org/10.1109/ROBOT.2003.1242106]

[6] R. J. Wood, E. Steltz, and R. S. Fearing, *Sens. Actuators, A*, **119**, 476 (2005). [DOI: https://doi.org/10.1016/j.sna.2004.10.024]

[7] M. H. Park, H. H. Chong, B. H. Lee, S. S. Jeong, and T. G. Park, *Ferroelectrics*, **500**, 218 (2016). [DOI: https://doi.org/10.1080/00150193.2016.1216228]

[8] D. Chen, X. H. Lu, T. H. Cheng, and H. Y. Li, *Proc. 2016 Symposium on Piezoelectricity, Acoustic Waves, and Device Applications (SPAWDA)* (IEEE, Xi'an, China, 2016) p. 403. [DOI: https://doi.org/10.1109/SPAWDA.2016.7830034]

[9] S. Ueha, Y. Tomikawa, M. Kurosawa, and N. Nakamura, *Ultrasonic Motors: Theory and Applications* (Clarendon Press, Oxford, 1993) p. 8.

[10] K. Spanner and B. Koc, *Actuators*, **5**, 6 (2016). [DOI: https://doi.org/10.3390/act5010006]